

# Structure and Electrical Properties of Grafted Polypropylene/Graphite Nanocomposites Prepared by Solution Intercalation

Jing-Wei Shen, Xiao-Mei Chen, Wen-Yi Huang

College of Polymer Science and Engineering, Sichuan University, Chengdu 610065, China

Received 11 January 2002; accepted 11 July 2002

**ABSTRACT:** A novel process was developed to prepare electrically conducting maleic anhydride grafted polypropylene (gPP)/expanded graphite (EG) nanocomposites by solution intercalation. The conducting percolation threshold at room temperature ( $\Phi_c$ ) of the nanocomposites was 0.67 vol %, much lower than that of the conventional conducting composites prepared by melt mixing ( $\Phi_c = 2.96$  vol %). When the EG content was 3.90 vol %, the electrical conductivity ( $\sigma$ ) of the former reached  $2.49 \times 10^{-3}$  S/cm, whereas the  $\sigma$  of the latter was only  $6.85 \times 10^{-9}$  S/cm. The TEM, SEM, and optical microscopy observations confirmed that the significant decrease of  $\Phi_c$  and the striking increase of  $\sigma$

might be attributable to the formation of an EG/gPP conducting multiple network in the nanocomposites, involving the network composed of particles with a large surface-to-volume ratio and several hundred micrometers in size, and the networks composed of the boards or sheets of graphite with high width-to-thickness ratio and particles of fine microscale or nanoscale sizes. © 2003 Wiley Periodicals, Inc. *J Appl Polym Sci* 88: 1864–1869, 2003

**Key words:** nanocomposites; conducting polymers; morphology

## INTRODUCTION

Electrically conductive polymer composites are of special interest in the realm of functional materials. Addition of diverse conducting fillers such as carbon black,<sup>1,2</sup> graphite,<sup>3</sup> and metal fiber or powder<sup>4</sup> into thermoplastic polymers (TP) through melt mixing is an effective approach to fabricate the composites. Because greater amounts of the fillers, generally >15 wt %, were required for the host polymer to become conductive, which resulted in both poor processability and bad mechanical properties, the application of these conventional composites was largely restricted.

Because the nylon 6/layered silicate (LS) nanocomposites were first prepared by intercalation polymerization in 1987, the research and applications of TP/LS nanocomposites have made striking progress, and have offered new insight and an innovative route in the preparation of highly conductive composites with excellent integrative properties. In the meantime, the techniques of graphite intercalation compound (GIC) developed very quickly,<sup>6</sup> providing a favorable premise for the research and advancement of TP/graphite conducting composites. Recently, Pan et al.<sup>7</sup> prepared nylon 6/expanded graphite (EG) conducting

nanocomposites by intercalation polymerization, which had a percolation threshold ( $\Phi_c$ ) of 0.75 vol % and an electrical conductivity ( $\sigma$ ) of  $10^{-4}$  S/cm at 2.0 vol % EG. This showed the tremendous potential and value of TP/EG conducting nanocomposites.

In view of the successful preparation of TP/LS nanocomposites by solution or melt intercalation, we attempted in this study to prepare maleic anhydride grafted polypropylene (gPP)/EG conducting nanocomposites by solution intercalation, in contrast to the conducting composites prepared by normal melt mixing.

## EXPERIMENTAL

### Materials

The graphite used in this study was an expandable graphite (LX-2053) with an average diameter of 300  $\mu\text{m}$  and an expanded volume of 250 mL/g, supplied from Baoding Lianxing Carbide Company (China). The maleic anhydride grafted polypropylene with a grafted ratio of 0.7–0.8 wt % and a melt index of 12 g/10 min was supplied from Nanjing Julong Chemical Company (China).

### Sample preparation

The expandable graphite was placed in an oven at 950°C for rapid expansion and exfoliation to obtain the expanded graphite (EG).

Correspondence to: J.-W. Shen (shenjw@stusc.edu.cn).

Contract grant sponsor: National Ministry of Education, China; contract grant number: 20010610031.

### Melt mixing (MM) method

The mixtures of gPP and EG were put into a mixing chamber of a Haake System-40 torque rheometer (Haake Buchler Co., USA) and mixed at 190°C and 30 rpm for 8 min, followed by compression molding at 190°C and 5 MPa for 2 min, with a YX-50 press (Shanghai Weili Rubber & Plastics Machine Co., China) to obtain plates with dimensions of 100 × 100 × 2 mm<sup>3</sup>.

### Solution intercalation (SI) method

The EG was dispersed in xylene to prepare a suspending dispersion with certain EG content. The gPP was dissolved in xylene by heating to a backflow temperature of xylene (about 130°C). The EG suspending dispersion was added drop by drop into the gPP solution at the backflow state. After a backflow of 1.5 h, on cessation of heating, a portion of xylene was extracted under vacuum during the cooling process. When the temperature decreased to about 70°C, the resultant mixture was precipitated by adding acetone, and then filtered and dried under vacuum. The resulting loose powder was pressed under the same conditions to obtain plates of the same size as in the MM method.

### Measurement of electrical conductivity

The volume conductivity ( $\sigma$ ) of the plate samples was measured at room temperature by a ZC36 high-resistance meter (Shanghai Precise Instrument & Meter Co., China) when the  $\sigma$  was less than 10<sup>-8</sup> S/cm, or by a DT9025 numeric multimeter (Shenzhen Zhongjia Instrument & Meter Co., China) when the  $\sigma$  was greater than 10<sup>-8</sup> S/cm. In the latter case, pieces of copper foil fastened with a conducting paste were used as the electrodes.

### TEM observation

A transmission electron microscope (JEM-100CX II, Kyoto, Japan) was used to observe the microstructure of the composites prepared by solution intercalation. Ultrathin samples were obtained by microtoming the frozen plates using an LKB ultramicrotome (LKB Ultrascan XL, Bromma, Sweden), equipped with a freezing chamber.

### SEM observation

Two scanning electron microscopes (Hitachi X-650 and Philips XL-30, Japan) were used to observe the morphology of EG and gPP/EG composites prepared by the MM and SI methods. The plate samples were freeze-fractured, and the fractured surfaces were etched with xylene vapor and then sputtered with gold.

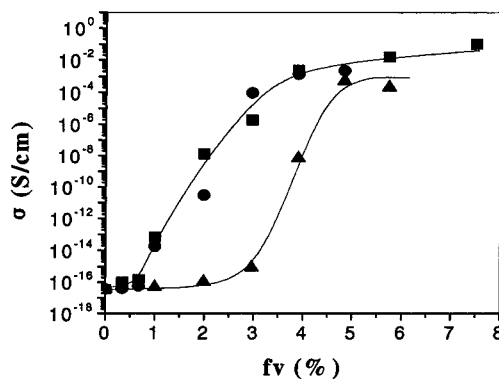


**Figure 1** Electrical conductivity ( $\sigma$ ) versus volume fraction of expanded graphite ( $f_v$ ) for gPP/EG composites prepared by two methods: melt mixing (▲); solution intercalation (■); solution intercalation, repeated experiment (●).

### Optical microscopy (om) observation

An optical microscope (Leitz Diaplan, Wetzlar, Germany) was used to observe the dispersed morphology of EG particles in the composites prepared by the two methods. Thin samples (1 mm thickness) were obtained by slicing the plates along the direction of thickness using a microtome. During observation, reflected polarizing light was used and the contrast ratio of visual field was adjusted by regulating the rotation angle of the polarizing prism to gain clear pictures, which were recorded by a microcomputer numeric picture-processing system.

## RESULTS AND DISCUSSION

### Conductibility

Figure 1 represents the volume conductivity ( $\sigma$ ) of gPP/EG composites, prepared by the MM and SI methods, as a function of EG volume fraction ( $f_v$ ). The  $f_v$  was calculated from the EG weight fraction, and the solid densities of EG and gPP were taken as 2.26<sup>8</sup> and 0.92 g/cm<sup>3</sup>, respectively. The percolation threshold ( $\Phi_c$ ) of the composites prepared by the SI and MM methods were 0.67 and 2.96 vol %, respectively, and the  $\Phi_c$  of the former was less than a quarter that of the latter. When the EG content was 3.90 vol %, the  $\sigma$  of the SI-prepared composite was  $2.49 \times 10^{-3}$  S/cm, which was 6 orders of magnitude higher than that of the MM-prepared composite ( $\sigma = 6.85 \times 10^{-9}$  S/cm). Moreover, the percolation region width of the SI-prepared composite ranged from 0.67 to 3.90 vol % EG, which was remarkably broader than that of the MM-prepared composite ( $f_v = 2.96$ –4.83 vol % EG). It is also worth noting that the  $\sigma$ – $f_v$  relation of the composites prepared by solution intercalation showed good repeatability.

### Morphology and internal microstructure

The expandable graphite used was a kind of graphite intercalation compound (GIC), fabricated from natural

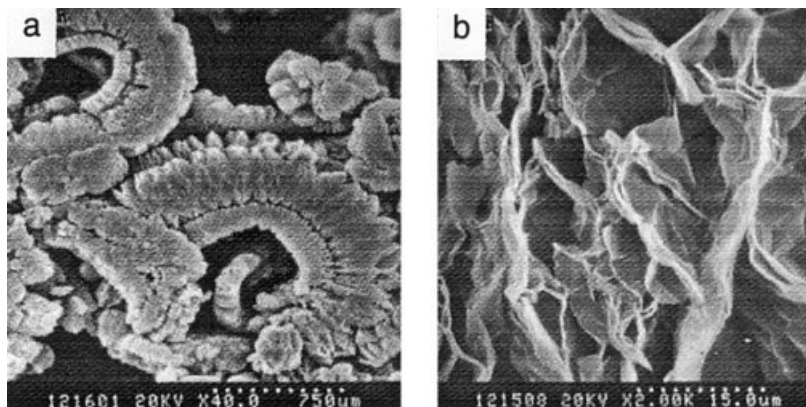


**Figure 2** SEM micrographs of expanded graphite showing (a) particle shape and (b) microstructure. Magnifications and scales: (a)  $\times 40$ , 750  $\mu\text{m}$ ; (b)  $\times 2.0\text{K}$ , 15  $\mu\text{m}$ .

flaky graphite (NFG) through chemical oxidation in the presence of concentrated sulfuric acid and nitric acid. The NFG is composed of layered, but compactly fastened nanosheets of graphite and is itself a good conductor, with  $\sigma = 10^4 \text{ S/cm}$ .<sup>9</sup> The GIC differs from the NFG and is itself a nanocomposite, containing intercalating agents and characterized by increased interplanar spacing. The EG obtained by rapid heating of the GIC had much greater interplanar spacing than that of GIC, and thus emerged in a loose and porous vermicular shape [Fig. 2(a)]. Its structure is basically parallel boards and sheets, which deform and collapse in an irregular pattern<sup>10</sup> and then form a networklike structure with many pores of varied sizes, ranging from nanoscale to microscale [Fig. 2(b)]. Thus, the galleries between the nanosheets of EG and pores in the EG network provide a larger space and can be easily intercalated by suitable monomers, catalysts, and even macromolecules.

Figure 3 shows the TEM photographs of the gPP/EG (1.99 vol %) composite prepared by solution intercalation, taken from different sites of the same ultrathin sample. The TEM observations were repeatable and representative. The black lines and the white domains are referred to as the exfoliated graphite sheets and the gPP matrix, respectively. Apparently, the graphite nanosheets with high aspect (width-to-

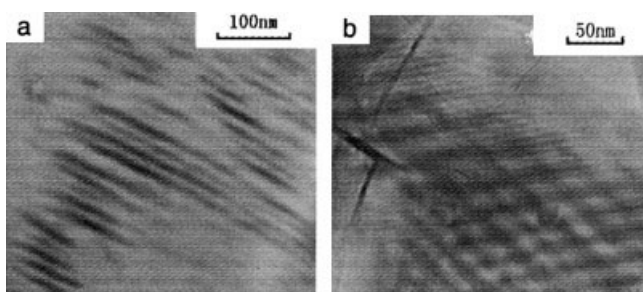


**Figure 3** TEM micrographs of gPP/EG (1.99 vol %) nanocomposite prepared by solution intercalation, taken from different sites of the same ultrathin sample.

thickness) ratio paralleled each other and possibly along different directions, and they had a thickness of about 10 nm and an interlayer spacing of about 30 nm. The microstructure formed here is similar to that observed by Pan et al.<sup>7</sup> in nylon 6/EG conducting nanocomposites prepared by intercalation polymerization. This indicates that the TP/EG conducting nanocomposites can be prepared not only by intercalation polymerization but also by solution intercalation.

Figure 4 shows the SEM photographs of gPP/EG (1.99 vol %) composites prepared by the two methods. It can be seen by comparison of Figure 4(a), (b) with Figure 2(b) that the internal structure of EG in the nanocomposite prepared by the SI method was roughly identical to that of the original EG (i.e., they both emerged in a network structure), but the pore size and the board thickness in the former were larger and thinner than those in the latter, respectively. This suggests that, although EG itself cannot bear a net charge because of its loose, porous and breakable features, it becomes solid after intercalating the gPP in it and then can basically maintain its original network structure during compression molding. Moreover, because the intercalation of gPP can promote the delamination and exfoliation of graphite boards and sheets as well as enlarge the space between them, the EG/gPP network formed had a larger size and finer structure than those of the original EG network, characterized by a greater aspect ratio of the sheets and boards. However, pronounced changes in the internal structure of EG took place in the composite prepared by the MM method [Fig. 4(c)]. The boards and sheets of graphite were severely bent and bundled and both the interplanar space and the pore sizes obviously diminished. This means that the original EG network was largely destroyed under stress because of the absence of gPP.

Figure 5 shows the OM photographs of gPP/EG (1.99 vol %) composites prepared by the two methods. It can be seen that the two preparation methods led to very different morphologies of the EG dispersed

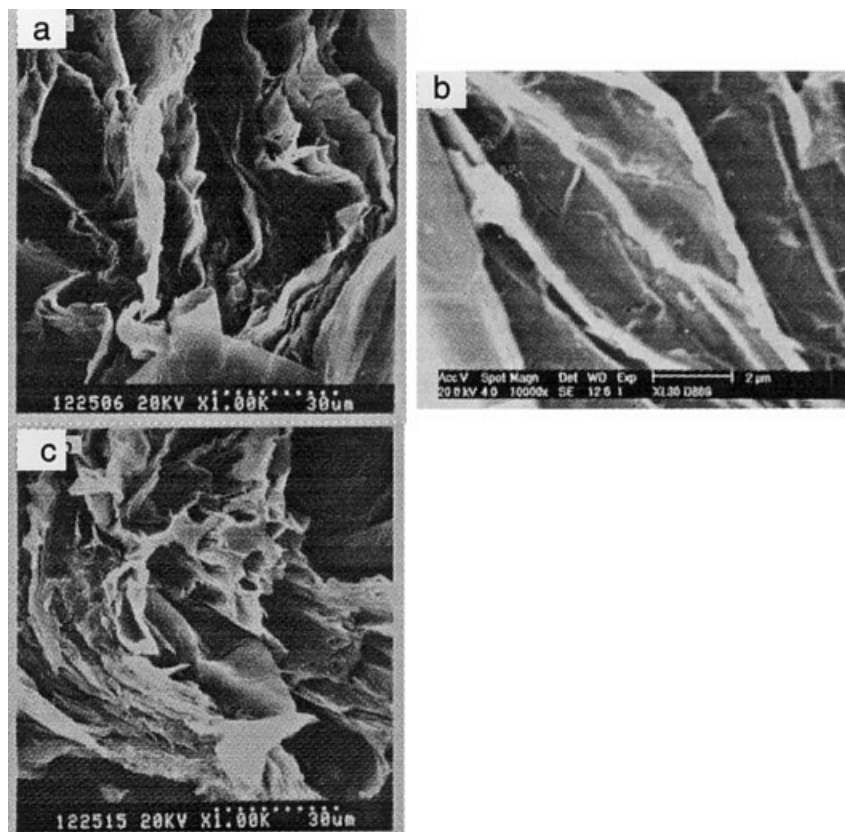


**Figure 4** SEM micrographs of gPP/EG (1.99 vol %) composites prepared by solution intercalation (a, b) and melt mixing (c). Magnifications and scales: (a)  $\times 1.0K$ , 30  $\mu m$ ; (b)  $\times 1.0K$ , 2  $\mu m$ ; (c)  $\times 1.0K$ , 30  $\mu m$ .

phase in the composites. In the nanocomposite [Fig. 5(a), (b)], the EG particles were characterized by a very large surface-to-volume ratio because of the presence

of gPP, such that they can abut and contact each other and then form a network. Contrarily, in the normal composite [Fig. 5(c), (d)], the EG particles with a small surface-to-volume ratio existed in the form of relatively isolated “islands” because of the absence of gPP and the breakable nature of EG itself.

The TEM, SEM, and OM observations mentioned earlier revealed the differences in the morphology and internal microstructure of the gPP/EG composites prepared by two methods from different structure levels. It can be concluded that the nanocomposites prepared by solution intercalation had an EG/gPP multiple network structure, which was composed of the particles, the boards or sheets, and the nanosheets with different scales. On the contrary, there was no such multiple network existing in the normal composites prepared by melt mixing. This can be attributed to the fact that during solution intercalation, the gPP molecules can more sufficiently intercalate the pores and galleries of EG through the solvation effect of xylene, the physical absorption of EG pores, and the polar interaction between the MAH groups of gPP and the  $-OH$  and  $-COOH$  groups on the EG sheets (resulting from chemical oxidation during the preparation of the GIC and EG<sup>11</sup>), driven by the solution flow at the boiling state and the extraction under vacuum. Moreover, as the intercalation process proceeded, the

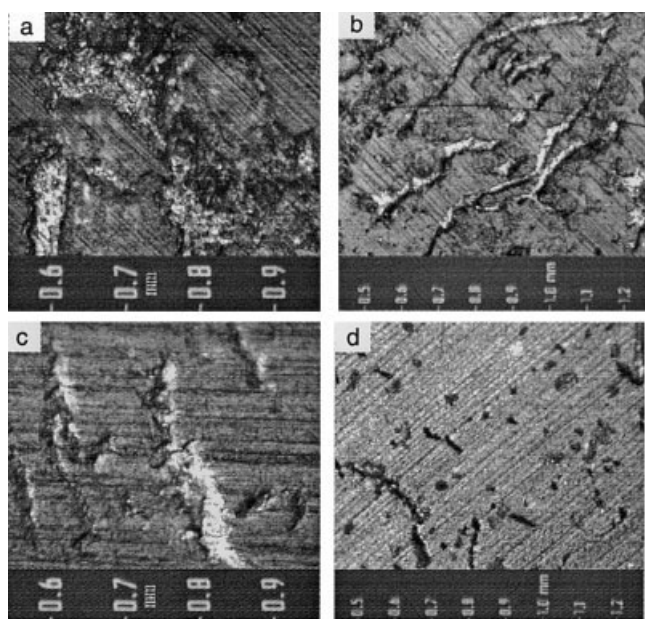


**Figure 5** OM photographs of gPP/EG (1.99 vol %) composites prepared by solution intercalation (a, b) and melt mixing (c, d), showing the morphological differences of the dispersed phase of EG.

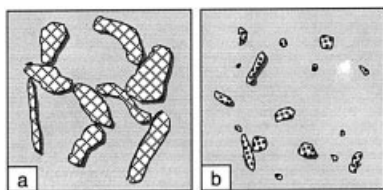


**Figure 6** Structural model of gPP/EG (1.0–2.96 vol %) composites prepared by solution intercalation (a) and melt mixing (b), showing the formation of conducting paths.

graphite boards and sheets might be further delaminated and exfoliated, which would allow more gPP molecules to intercalate and enlarge the space between them. Thus, the intercalated gPP can support, improve, and solidify the formed EG/gPP network, thus preventing the network from destruction under stress. Compared with the case mentioned above, the gPP molecules that entangled each other in the highly viscous melt cannot intercalate the spacing between the sheets of EG under shear stress or compression; at most, they can infiltrate only the larger pores of EG. Consequently, the original EG network was destroyed to a large extent under the stress.

#### Formation of conducting paths

The electrically conducting mechanism of polymer composites is associated with two questions: (1) how to form the conducting paths and (2) how to conduct after the formation of the paths. Concerning the second question, several theories exist, such as contact conducting, the tunneling effect, dielectric breakdown, and field emission. It is generally believed that conductivity depends on their combined effect and could be summarized by the general statement that the microscopic migration of electrons might have several mechanisms. With regard to the first question, there are, for example, the percolation theory,<sup>12</sup> the effective medium theory,<sup>13</sup> the microstructure theory,<sup>14</sup> and the thermodynamic theory.<sup>15</sup> These theories all relate to the dispersed morphology and internal microstructure of conducting fillers in polymer matrices, which depend on geometrical, thermodynamic, and dynamic factors such as the nature of filler and polymer, formulation, preparation methods, and processing conditions. Hence, the formation mechanism of conducting paths is related to the fact that the conducting filler particles with different morphologies and internal microstructures can form the paths by distinct ways or patterns.

For the gPP/EG conducting composites investigated in this study, according to their  $\sigma$ - $f_v$  relations as shown in Figure 1, the percolation theory can be introduced to focus on the formation mechanism of conducting paths. As for the composites with lower EG contents ( $f_v = 1.0$ – $2.96$  vol %), the model illustrated in Figure 6 can be used to interpret it.

For the nanocomposites prepared by solution intercalation [Fig. 6(a)], the EG particles with a large surface-to-volume ratio can abut or contact and then form a conducting path network at lower EG contents, resulting from the intercalation of gPP into them and thus forming EG/gPP nanoscale and microscale networks, which protect the EG particles from destruction during compression. Therefore, the percolation threshold ( $\Phi_c$ ) of the nanocomposites was remarkably low. Moreover, given that the formation of the EG/gPP multiple network including the particle network was a process of gradual development with the increase of EG contents, the percolation region was actually wider.

As to the normal composites prepared by melt mixing [Fig. 6(b)], the EG particles were broken up during processing and their sizes and the surface-to-volume ratios decreased drastically. Consequently, only at higher EG contents can they abut or contact and form the conducting paths; thus the  $\Phi_c$  of the composites was quite high. Simultaneously, the formation of the conducting paths composed of small and compacted EG particles must occur in a narrow range of EG contents, so the percolation region was relatively narrow.

#### CONCLUSIONS

A new process was developed to prepare the gPP/EG electrically conductive nanocomposites by solution intercalation. In contrast with the conventional composites prepared by melt mixing, the percolation threshold ( $\Phi_c$ ) of the nanocomposite ( $\Phi_c = 0.67$  vol %) was less than a quarter that of the normal composites ( $\Phi_c = 2.96$  vol %), and when the EG content was 3.90 vol %, the electrical conductivity ( $\sigma$ ) of the former ( $\sigma = 2.49 \times 10^{-3}$  S/cm) was 6 orders of magnitude higher than that of the latter ( $\sigma = 6.85 \times 10^{-9}$  S/cm). The TEM, SEM, and OM observations confirmed that an EG/gPP multiple network structure was formed in the nanocomposites, including the network composed of the particles with large surface-to-volume ratio and several hundred micrometers in size, and the networks composed of the boards or sheets of graphite with high width-to-thickness ratio and particles of fine microscale or nanoscale sizes. Only the multiple network played a deciding role in the great improvement of electrical conductivity of the nanocomposites.

The authors gratefully acknowledge the support of Doctoral Research Foundation granted by the National Ministry of Education, China (Grant 20010610031). Special thanks are also due to the State Key Laboratory of Polymer Materials Engineering, Sichuan University for the structural characterizations.

#### References

1. Tan, H.; Liu, Z. Y.; Lou, X. F.; Li, S. H. *J Appl Polym Sci* 1994, 51, 1159.

2. Tchoudakov, R.; Breur, O.; Narkis, M.; Siegmann, A. *Polym Eng Sci* 1996, 36, 1336.
3. Nagata, K.; Iwabuki, H.; Nigo H. *Compos Interface* 1999, 6, 483.
4. Sun, J. S.; Gokturk, H. S.; Kalyon, D. M. *J Mater Sci* 1993, 28, 364.
5. Zweifel, Y.; Plummer, C. J. G.; Kausch, H. H. *J Mater Sci* 1998, 33, 1715.
6. Novel, M.; Santhanam, R. *J Power Sources* 1998, 72, 53.
7. Pan, Y.-X.; Yu, Z.-Z.; Qu, Y.-C.; Hu, G.-H. *J Polym Sci Part B: Polym Phys* 2000, 38, 1626.
8. Ishigure, Y.; Iijima, S.; Ito H. *J Mater Sci* 1999, 34, 2979.
9. King, J. A.; Tucker, K. W.; Vogt, B. D.; Weber, E. H.; Quan, C. L. *Polym Compos* 1999, 20, 643.
10. Cao, N.; Shen, W.; Wen, S.; Liu, Y. *New Carbon Mater* 1995, 4, 51.
11. Kotov, N. A.; Dekany, I.; Fendler, J. H. *Adv Mater* 1996, 8, 637.
12. Zhang, C.; Yi, X.; Yui, H.; Asai, S.; Sumita, M. *J Appl Polym Sci* 1998, 69, 1813.
13. Mclachlan, D. S. *J Phys C: Solid State Phys* 1988, 21, 1521.
14. Weber, M.; Kamal, M. R. *Polym Compos* 1997, 18, 711.
15. Lux, F. *J Mater Sci* 1993, 28, 285.